XPS and LEED study of a single-crystal surface of pyrite

S. Chaturvedi,[1] R. Katz,[1] J. Guevremont,[1] M.A.A. Schoonen,[2] and D.R. Strongin[1]

[1]Department of Chemistry, State University of New York, Stony Brook, NY 11794, U.S.A.
[2]Department of Earth and Space Sciences, State University of New York, Stony Brook, NY 11794, U.S.A.

Abstract

This work reports X-ray photoelectron spectroscopy (XPS) and low-energy electron diffraction (LEED) results for an as-grown (100) surface of pyrite (FeS_2) cleaned by low-energy He^+ ion bombardment and thermal annealing. LEED suggests that the atomically clean pyrite surface prepared in this manner is unreconstructed. XPS S 2p data for this surface show no evidence for a monosulfide species coexisting with the disulfide moiety that characterizes pyrite. This experimental observation contrasts with many prior studies that prepared pyrite surfaces by cleavage or mechanical cutting and observed a monosulfide species. We argue that a pyrite surface prepared directly from the as-grown surface may better represent a natural surface than does a preparation method such as cleavage.

Introduction

Historically, surface science studies in the physics and chemistry communities have been geared in large part to understanding surface-mediated processes such as catalysis, corrosion resistance, and methods for information processing and storage (Somorjai 1994) on metal and semiconductor surfaces. By comparison, much less research effort has been expended on developing a similar molecular-level understanding of macroscopic phenomena that occur on geological materials. In fact, this area is relatively unexplored with modern surface science techniques, even though surface-mediated chemical reactions on geological materials partake in many environmental processes ranging from erosion to mineral formation (Hochella and White 1990), as well as the sorption of organic molecules (Kriegman-King and Reinhard 1994) and catalysis (Xu and Schoonen 1995; Hochella 1995).

We recently became intrigued about using an array of modern surface science techniques to develop a molecular-level understanding of how environmentally relevant molecules chemisorb and react on 3d transition metal disulfides. As a necessary first step in developing a molecular-level understanding of geochemical reactions on minerals using ultra-high vacuum (UHV) spectroscopic techniques, it is imperative to study surfaces that occur in the environment and that have a known stoichiometry and structure [properties of the surface that dictate its reactivity (Somorjai 1994)]. The purpose of this paper is to report initial X-ray photoelectron spectroscopy (XPS) and low-energy electron diffraction (LEED) data for an atomically clean (100) face of pyrite, FeS_2, prepared directly from an as-grown surface.

Experimental methods

All experiments were performed in a bakeable UHV chamber, which was evacuated with turbomolecular, ion, and titanium sublimation pumps. The experimental chamber had a typical working base pressure of 3×10^{-10} torr. It was equipped with a quadrupole mass spectrometer (UTI, 100C), front-view LEED optics (Perkin-Elmer, 15-120), double-pass cylindrical mirror analyzer (CMA, Perkin-Elmer, 15-255G), and X-ray source (Perkin-Elmer, 04-548). The CMA contained a coaxial electron gun to perform Auger electron spectroscopy (AES). An ion gun (Perkin-Elmer, 04-161) in the chamber was used for sample cleaning.

The pyrite used in this research is from Huanzala, Peru. The sample from which data were obtained was a 2 mm thick square plate with an area of 1 cm^2. The plate was cut from a 6 cm^3 irregularly shaped pyrite crystal. It is important to note, however, that one side of the plate was an as-grown surface, and the sample was handled carefully to avoid any mechanical or chemical alteration of this natural surface outside the UHV chamber. Laue back reflection patterns of the sample before it was placed into the UHV chamber showed sharp diffraction spots, and their symmetry indicated that the exposed face was of (100) orientation. The pyrite plate was mounted on a tantalum foil with a conductive ceramic cement (Ag was a component). This whole assembly was held in contact with a liquid nitrogen cryostat using tantalum wires spot-welded to the foil and mechanically clamped (electrically isolated) to the cryostat. Cooling down to 135 K was routinely achieved. The sample was resistively heated by passing current through the support wires. The temperature of the crystal was monitored with a type-K thermocouple, which was attached to the back of the sample using the thermally conductive ceramic cement.

XPS was performed by using the Mg$K\alpha$ line (1253.6 eV) as the excitation source. X-rays used in this research were unmonochromatized. S 2p and Fe 2p core-level data were obtained by using a CMA pass energy of 25 eV. All binding energies were referenced to the sample Fermi lev-
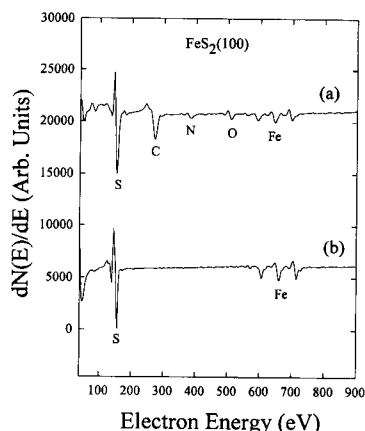
FIGURE 1. AES spectrum of the naturally occurring (100) face of FeS$_2$ (a) prior to cleaning and (b) after cleaning cycles of He$^+$ bombardment and 573 K annealing. A total of ~3 h of sputter time was needed to remove the contamination.

el. The spectrometer was calibrated over a wide range of kinetic energies by considering the position of the Fermi-level cutoff when using the MgKα line and He I radiation (21.2 eV) and by obtaining the binding energies for a variety of pure metals in the spectrometer (Fe, Ni, Co, and Ti). Repeated data acquisitions for the S and Fe 2p levels show that the quoted binding energies in this paper have an uncertainty of ±0.3 eV.

AES was performed with a 3000 eV electron beam. Sample current during AES was typically on the order of 1 μA. The AES spectra presented are given in the derivative mode [i.e., dN(E)/dE]. A modulation voltage with an amplitude of 3 V and a frequency of 1 kHz was placed on the outer cylinder of the CMA to obtain these data.

Figure 1 exhibits an AES spectrum of the pyrite plate. Major contaminants bound on the as-grown surface are C, N, and O. Simple annealing of the crystal up to 573 K leads to no noticeable changes in the level of contamination as judged by AES. This untreated crystal surface produces no LEED pattern.

Figure 1b exhibits an AES spectrum of FeS$_2$ (100) subsequent to in situ cleaning, showing that the C, N, and O contamination was removed from the surface. An XPS analysis indicates that the ratio of S to Fe in the near-surface region is 1.9:1.0 ± 0.2, which is consistent with the 2:1 ratio expected for a stoichiometric pyrite sample. The cleaning procedure used in this case consisted of multiple ion bombardment and anneal cycles. The important point here, which distinguishes this procedure from the typical sputter cleaning procedure used in the surface science community, is that He$^+$ was used as the bombarding ion rather than Ne$^+$ or Ar$^+$. Furthermore, the kinetic energy of the ion was kept at 200 eV (ion beam was set at 500 eV and the sample was biased to 300 V above ground potential). The actual cleaning cycle consisted of ~10 min of sputtering followed by annealing at 573 K for ~5 min. Approximately ten cycles of this treatment produced the AES spectrum presented in Figure 1b.

During this cleaning procedure the S:Fe AES intensity ratio was nearly constant, suggesting that the He$^+$ bombardment did minimal damage to the surface except for slow removal of the loosely bound C, N, and O contamination. Without annealing, however, a LEED pattern could not be obtained, indicating that some damage to the long-range order of the surface by the ion bombardment could not be avoided. Presumably, most of the damaged surface was recovered by the annealing. We note that annealing is typically a component of any UHV cleaning method involving ion bombardment. Such a thermal treatment may be useful in removing imperfections produced by mechanical cutting or breakage methods used to prepare samples. For our experiments, anneal temperatures higher than 500 K were needed to produce the ordered (100) surface of pyrite (the temperature was never increased above 623 K) as judged from LEED observations. Ion bombardment with 500 eV He$^+$ coupled with annealing was also investigated as a cleaning procedure. This method produced a similar ordered surface, but prolonged cleaning cycles using this ion energy started to degrade the sample structure. This degradation was evident by an enhanced background in the LEED pattern and by a loss in the metallic-like luster of the pyrite surface.

In addition to He$^+$ cleaning, experiments were performed in which the naturally occurring surface was bombarded with 500 eV Ar$^+$ ions. This bombardment, coupled with annealing at 573 K, removed the C and O contamination much more rapidly than either of the He$^+$ cleaning procedures. The surface stoichiometry of the pyrite surface, however, was altered more by Ar$^+$ bombardment than by the methods employing the He$^+$ ion. This circumstance was made evident by the observation that after Ar$^+$ bombardment, the S Auger intensity was approximately equal to that of the Fe intensity. The 2:1 ratio of S:Fe could be recovered by annealing, but the geometric structure of the surface was irreparably damaged, as inferred from the inability to obtain a LEED pattern from this surface. We note that prior research (Raikar and Thurgate 1991) investigated the initial stages of oxidation of pyrite cleaned in UHV by similar Ar$^+$ ion bombardment methods. Although information about the long-range structure of the sample was not given, our present results suggest that this earlier work probably obtained results from a clean but poorly ordered surface. Consistent with this is research by Hochella et al. (1988) that showed that bombardment of mineral surfaces (e.g., quartz and albite) with Ar$^+$ leads to extensive structural modification. Sulfides are not expected to be an exception.

It is important to note that we were only able to produce clean and ordered (100) surfaces when the He bombardment and anneal method was used for the as-grown surfaces. We were never able to obtain a LEED pattern for a polished or unpolished pyrite surface that was cut with a diamond saw. Although bombardment and annealing of polished and unpolished cut surfaces lead to
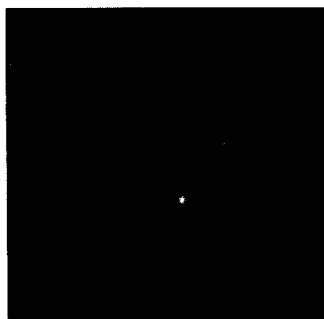
FIGURE 2. LEED pattern obtained from a clean FeS_2 (100) surface at an electron-beam energy of 125 eV. The middle [(0,0) beam] and left portions of the pattern are obscured by the sample holder.

Binding Energy (eV)

FIGURE 3. S 2p XPS spectra of FeS_2 (100). The upper spectrum is the raw data (dot-dash line is associated with the background), and the lower spectrum was obtained after background subtraction. Regions A and B are discussed in the text.

stoichiometric FeS_2 surfaces, the long-range order of the outermost surface appears to become permanently destroyed.

RESULTS AND DISCUSSION

Figure 2 exhibits a typical LEED pattern of the FeS_2 surface prepared using the procedure described above. The spots are fairly sharp and are similar to the pattern obtained by Pettenkofer et al. (1991) from FeS_2 (100) created by in situ cleavage. The same LEED pattern is obtained from the entire 1 cm^2 as-grown pyrite surface, indicating that the surface structure is rather homogeneous over the entire FeS_2 (100) sample. Cleavage of pyrite generally leads to conchoidal fracture (Wersin et al. 1994), and it was not mentioned in the earlier LEED study whether the geometric structure was of (100) orientation over the entire cleaved surface. Pettenkofer et al. (1991) concluded that the surface of FeS_2 (100) is in registry with the bulk. Our LEED pattern is consistent with this prior assertion. Qualitative examination of our LEED pattern as a function of incident energy suggests that the surface is unreconstructed, as inferred from the symmetry and by the absence of extra spots or splitting of spots throughout the 50–200 eV range. Quantitative LEED calculations (i.e., intensity vs. voltage) are required to verify this tentative conclusion. The as-grown surfaces of pyrite used in our study are not expected to be atomically smooth. Undoubtedly, these surfaces exhibit imperfections, such as steps and striations that contribute to the diffuse background in the LEED pattern.

Figure 3 exhibits S 2p photoemission data for clean and ordered FeS_2 (100). The top S 2p spectrum is the raw or unprocessed data, whereas the bottom spectrum was obtained using a background-subtraction method that accounts for the contribution of inelastically scattered electrons (Shirley 1972). We mention for completeness that although we concentrate on the S 2p photoemission data in this paper, the binding energy of the Fe $2p_{3/2}$ level of our pyrite sample was measured at 707.5 eV. This binding energy is approximately 0.5 eV higher than that quot-
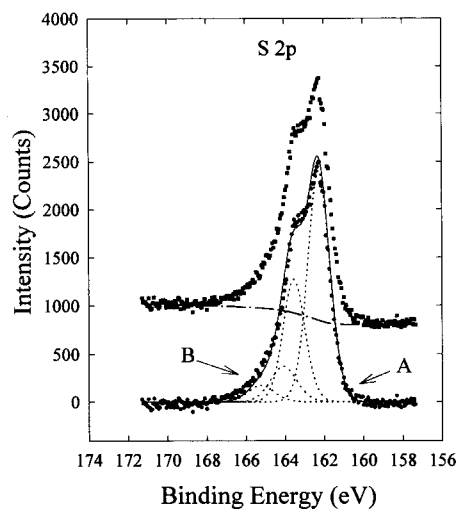
ed in the literature for the Fe $2p_{3/2}$-level pyrite (e.g., see Nesbitt and Muir 1994). The reason for this discrepancy is not known, but our value is reasonable considering that Fe metal exhibits core-level binding energies ~0.5 eV lower than the same levels of the more oxidized Fe in pyrite. [The $2p_{3/2}$ level of Fe metal was measured by our spectrometer (calibrated by the method described before) at 706.8 eV (Gleason and Strongin 1993), consistent with literature values for this metal.]

The S 2p data (Fig. 3, bottom spectrum) were fitted with two sets of curves derived from Lorentzian (20%) and Gaussian (80%) product peaks. The two largest curves, centered at 162.3 and 163.5 eV [FWHM (full-width half-maximum) = 1.3 eV], are assigned to the $2p_{3/2}$ and $2p_{1/2}$ core levels, respectively, of S, bound as disulfide groups in pyrite. The second set of peaks, centered at 164.1 and 165.2 eV (FWHM = 1.6 eV), are needed to fit the high–binding energy region of the S 2p data, and their interpretations are briefly discussed below. Constraints imposed on each peak set are an area ratio of 2:1 (i.e., doublet) and an equal peak width.

It is interesting to compare our S 2p results to analogous data obtained from pyrite surfaces produced by cleavage (Mycroft et al. 1990; Nesbitt and Muir 1994; Knipe et al. 1995) and mechanical cutting (Mycroft et al. 1995). The spectra obtained from samples prepared by cleavage or cutting typically exhibit features at the low-binding energy side (~161.5 eV) of the S $2p_{3/2}$ feature owing to emission from S_2 groups. This additional feature is commonly associated with the presence of monosulfide (Bronold et al. 1993; Nesbitt and Muir 1994). Inspection of our data in region A in Figure 3 shows the absence of spectral weight that can reasonably be attributed to a reduced form of S. The resolution of our spectra is quite modest, but we do not believe this can lead to the loss of

a low–binding energy feature. We cannot rule out, however, that our preparation method removed a monosulfide impurity in the pyrite that may exist on the surface in nature. It is also possible that the presence of monosulfide is a remnant of the cleavage or cutting process and is not associated with the natural growth surface. In the case of cleavage, a surface with significant defect density and inhomogeneous chemical structure is expected to result. We stress, however, that caution is necessary in any case in which the spectral weight in the S 2p region is assigned to a minority S species because the core-level binding energy of a surface species on pyrite can be different from that of a similar species in the bulk (Bronold et al. 1994).

Examination of the S 2p data in region B in Figure 3 shows that spectral weight, in addition to what we have attributed to disulfide emission, is present at high binding energy. Previous research has associated polysulfidic species with spectral weight in this high–binding energy region (Nesbitt and Muir 1994), and the S 2p doublet that we used to fit our data might be associated with such a species. However, we note that inelastically scattered electrons and final-state effects in the photoemission process (as well as deficiencies in the background removal process) may contribute to the high–binding energy side of the S 2p data. In the case of metals (Doniach and Sunjic 1970) similar processes result in asymmetries to the high–binding energy side of core levels (e.g., Fe 2p), and effects such as these may also contribute to the asymmetry of the S 2p spectrum obtained for pyrite. Therefore, we are not convinced that an additional sulfur species is present in the near-surface region of pyrite prepared by our method; if it is present, it is probably not responsible for the entire additional spectral weight in region B of Figure 3.

Intrinsic to any preparation technique is an alteration of the natural surface. Therefore, FeS$_2$ (100) prepared by the method described in this contribution cannot be directly associated with a natural surface. We believe, however, that our method offers at least two advantages over more conventional preparation techniques, such as cleavage. First, our method for preparing the cube face of pyrite results in the retention of the expected (100) long-range structure order over the entire surface. Second, our method yields a reproducible surface, a property that is important for experiments designed to elucidate the surface reactivity of pyrite (or any mineral).

ACKNOWLEDGMENTS

REFERENCES CITED

Bronold, M., Büker, K., Kubala, S., Pettenkofer, C., and Tributsch, H. (1993) Surface preparation of FeS$_2$ via electrochemical etching and interface formation with metals. Physica Status Solidi A, 135, 231–243.

Bronold, M., Tomm, Y., and Jaegermann, W. (1994) Surface states of cubic d-band semiconductor pyrite (FeS$_2$). Surface Science Letters, 314, L931–L936.

Doniach, S., and Sunjic, M. (1970) Many-electron singularity in X-ray photoemission and X-ray line spectra from metals. Journal of Physics, C3, 285–291.

Gleason, N.R., and Strongin, D.R. (1993) A photoelectron spectroscopy and thermal desorption study of CO on FeAl(110) and polycrystalline TiAl and NiAl. Surface Science, 295, 306–318.

Hochella, M.F., Jr. (1995) Mineral surfaces: Their characterization and their chemical, physical and reactive nature. Mineralogical Society Series, 5, 17–60.

Hochella, M.F., Jr., Lindsay, J.R., Mossotti, V.G., and Eggleston, C.M. (1988) Sputter depth profiling in mineral-surface analysis. American Mineralogist, 73, 1449–1456.

Hochella, M.F., Jr., and White, A.F. (1990) Mineral-water interface geochemistry. In Mineralogical Society of America Reviews in Mineralogy, 23, 1–16.

Knipe, S.W., Mycroft, J.R., Pratt, A.R., Nesbitt, H.W., and Bancroft, G.M. (1995) X-ray photoelectron spectroscopic study of water adsorption on iron sulphide minerals. Geochimica et Cosmochimica Acta, 59, 1079–1090.

Kriegman-King, M.R., and Reinhard, M. (1994) Transformation of carbon tetrachloride by pyrite in aqueous solution. Environmental Science and Technology, 28, 692–700.

Mycroft, J.R., Bancroft, G.M., McIntyre, N.S., Lorimer, J.W., and Hill, I.R. (1990) Detection of sulphur and polysulphides on electrochemically oxidized pyrite surfaces by X-ray photoelectron spectroscopy and Raman spectroscopy. Journal of Electroanalytical Chemistry, 292, 139–152.

Mycroft, J.R., Bancroft, G.M., McIntyre, N.S., and Lorimer, J.W. (1995) Spontaneous deposition of gold on pyrite from solutions containing Au(III) and Au(I) chlorides: Part I. A surface study. Geochimica et Cosmochimica Acta, 59, 3351–3365.

Nesbitt, H.W., and Muir, I.J. (1994) X-ray photoelectron spectroscopic study of a pristine pyrite surface reacted with water vapor and air. Geochimica et Cosmochimica Acta, 58(21), 4667–4679.

Pettenkofer, C., Jaegermann, W., and Bronold, M. (1991) Site specific surface interaction of electron donors and acceptors on iron disulfide (100) cleavage planes. Berichte der Bunsen Gesellschaft für physikalische Chemie, 95(5), 560–565.

Raikar, G.N., and Thurgate, S.M. (1991) An Auger and EELS study of oxygen adsorption on FeS$_2$. Journal of Physics: Condensed Matter, 3, 1931–1939.

Shirley, D.A. (1972) High-resolution X-ray photoemission spectrum of the valence bands of gold. Physical Review B, 5, 4709–4714.

Somorjai, G.A. (1994) Introduction to surface chemistry and catalysis, 667 p. Wiley, New York.

Wersin, P., Hochella, M.F., Jr., Persson, P., Redden, G., Leckie, J.O., and Harris, D.W. (1994) Interaction between aqueous uranium (VI) and sulfide minerals: Spectroscopic evidence for sorption and reduction. Geochimica et Cosmochimica Acta, 58, 2829–2843.

Xu, Y., and Schoonen, M.A.A. (1995) The stability of thiosulfate in the presence of pyrite in low-temperature aqueous solutions. Geochimica et Cosmochimica Acta, 59, 4605–4622.